Proceedings of the ASME 2010 International Design Engineering Technical Conferences &
Computers and Information in Engineering Conference
IDETC/CIE 2010
August 15-18, 2010, Montreal, Quebec, Canada

DETC2010/DAC-28064

A MINLP MODEL FOR GLOBAL OPTIMIZATION OF PLUG-IN HYBRID VEHICLE DESIGN AND ALLOCATION TO MINIMIZE LIFE CYCLE GREENHOUSE GAS EMISSIONS

Ching-Shin Norman Shiau
Research Assistant
Mechanical Engineering
Carnegie Mellon University
Pittsburgh, Pennsylvania 15213
cshiau@cmu.edu

Jeremy J. Michalek*
Associate Professor
Mechanical Engineering
Engineering and Public Policy
Carnegie Mellon University
Pittsburgh, Pennsylvania 15213
jmichalek@cmu.edu
* Corresponding Author

ABSTRACT

Plug-in hybrid electric vehicles (PHEVs) have potential to reduce greenhouse gas (GHG) emissions in the U.S. light-duty vehicle fleet. GHG emissions from PHEVs and other vehicles depend on both vehicle design and driver behavior. We pose a twice-differentiable, factorable mixed-integer nonlinear programming model utilizing vehicle physics simulation, battery degradation data, and U.S. driving data to determine optimal vehicle design and allocation for minimizing lifecycle greenhouse gas (GHG) emissions. The resulting nonconvex optimization problem is solved using a convexification-based branch-and-reduce algorithm, which achieves global solutions. In contrast, a randomized multistart approach with local search algorithms finds global solutions in 59% of trials for the two-vehicle case and 18% of trials for the three-vehicle case. Results indicate that minimum GHG emissions is achieved with a mix of PHEVs sized for around 35 miles of electric travel. Larger battery packs allow longer travel on electric power, but additional battery production and weight result in higher GHG emissions, unless significant grid decarbonization is achieved. PHEVs offer a nearly 50% reduction in life cycle GHG emissions relative to equivalent conventional vehicles and about 5% improvement over ordinary hybrid electric vehicles. Optimal allocation of different vehicles to different drivers turns out to be of second order importance for minimizing net life cycle GHGs.

1. INTRODUCTION[1]

Plug-in hybrid electric vehicle (PHEV) is a promising technology for addressing the issues of foreign oil dependency and global warming within the U.S. transportation sector [2]. PHEVs are similar to ordinary hybrid electric vehicles (HEVs), except the PHEV carries a larger battery pack and offers plug-charging capability [3]. PHEVs use large battery packs to store energy from the electricity grid and propel the vehicle partly on electricity instead of gasoline. Under the average mix of electricity sources in the U.S., vehicles can be driven with lower operation cost and fewer greenhouse gas (GHG) emissions per mile when powered by electricity rather than by gasoline [4]. PHEVs have the potential to displace a large portion of gasoline consumed by the transportation, since approximately 60% of daily U.S. passenger vehicle trips are less than 30 miles [5].

We focus our design study on PHEVs with an all-electric control strategy[2], which disables engine operation in charge-depleting mode (CD mode) and draws propulsion energy entirely from the battery until it reaches a target state of charge (SOC) [3]. Figure 1 shows the battery energy status in PHEV operation. The distance that a PHEV can travel on electricity alone with a fully charged battery is called its all-electric range (AER).[3] Battery swing is the window between maximum SOC and target SOC, which is determined by the control strategy, and we base our swing definition on percent of cell energy used, rather than percent of SOC. Once the driving distance reaches the AER and the battery is depleted to the target SOC, the PHEV switches to operate in charge-sustaining mode (CS mode), and the gasoline engine provides energy to propel the vehicle and maintain battery charge near the target SOC. In CS mode, the PHEV operates similar to an ordinary HEV.

[1] We focus here on global optimization formulation and methodological contributions, and we leave examination of cost, petroleum consumption, sensitivity analysis, and policy implications to a companion paper [1].

[2] A blended-strategy PHEV uses a mix of the electric motor and gasoline engine to power the vehicle in CD-mode, while an all-electric PHEV uses only electricity. We confine our scope to all-electric strategy for simplicity, since blended-strategy operation characteristics are sensitive to control parameters.

[3] AER is defined as energy-equivalent electric distance for blended-mode PHEVs, but we consider only all-electric PHEVs in this study [6].

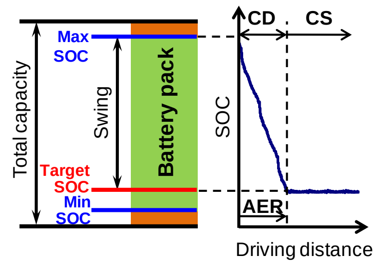

Figure 1. Battery energy status in CD- and CS-mode operation

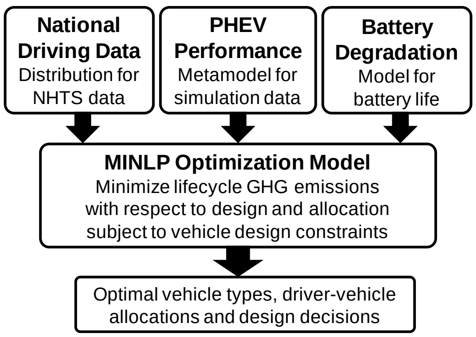

Figure 2. Framework of optimal PHEV design and allocation

We pose a benevolent dictator optimization model to determine optimal vehicle type, design, and allocation for achieving the social objective of minimum lifecycle GHG emissions from personal transportation.[4] Figure 2 provides an overview of the modeling framework, where three major components, national driving data, PHEV performance and battery degradation, form the bases of the optimization model.

Due to the combined nonlinearities in the driving data, the performance meta-model and the battery degradation model, the optimization problem is nonconvex and contains a mixture of continuous and discrete variables. The discrete variables corresponding to vehicle type are few in number and can be handled through exhaustive enumeration if necessary, producing a series of nonconvex nonlinear programs (NLPs). There are three primary approaches for solving nonconvex NLPs: (1) use a local NLP solver to find local solutions and invoke random multistart to seek global solutions [7]; (2) use a stochastic algorithm such as genetic algorithms or simulated annealing [8], or (3) use deterministic global optimization methods. Methods in group (1) and (2) are easy to implement, but they do not guarantee global solutions in finite time, and comparison of solutions across cases in sensitivity analysis is subject to uncertainty in attainment of global solutions in each sensitivity case. Methods in group (3) include gradient-based and derivative-free algorithms. Derivative-free deterministic global search algorithms that use partitioning, such as DIRECT, perform well only in low dimensional spaces (< 10 variables) and can perform poorly on constrained problems [9]. In contrast, gradient-based global solvers, such as BARON, can produce global solutions for significantly larger problems, but they require that objective and constraint functions be twice differentiable, factorable algebraic functions so that valid convex underestimation functions can be automatically constructed in nodes of the branch and bound tree [10].

We formulate our problem as a twice-differentiable, factorable MINLP that can be solved using BARON to ensure global solutions while managing both continuous and discrete variables. In Section 2, we first develop the formulation with specific models for the objective and constraint functions by specifying the distribution of miles driven per day, vehicle performance models, and the objective and constraint formulations. We then reformulate the model as a factorable, algebraic nonconvex MINLP that can be solved globally. In Section 3, we report solutions for minimum GHG emissions and compare the solution performance to the multi-start method with a local NLP solver. We then conclude in Section 4.

[4] We model allocation of vehicles to drivers as a dictated assignment based on driver daily travel distance and do not model market mechanisms. As such, we find the best possible outcome for GHG emissions, which is a lower bound for market-based outcomes.

2. MODEL

To optimize a single vehicle for minimum GHG emissions over the population of drivers, we minimize the integral of $f_O(\mathbf{x},s)$, the GHG emissions per day for vehicle design $\mathbf{x}$ when driven s miles per day, times the probability density function of daily driving distance $f_S(s)$ over the population of drivers.

$$\begin{aligned} &\underset{\mathbf{x}}{\text{minimize}} \int_0^\infty f_O(\mathbf{x},s)\, f_S(s)\, ds \\ &\text{subject to } \mathbf{g}(\mathbf{x}) \le \mathbf{0};\ \ \mathbf{h}(\mathbf{x}) = \mathbf{0} \end{aligned} \tag{1}$$

where $\mathbf{g}(\mathbf{x})$ is a vector of inequality constraints and $\mathbf{h}(\mathbf{x})$ is a vector of equality constraints ensuring a feasible vehicle design. We assume each vehicle is charged once per day, so that s indicates the distance traveled between charges.

To extend this model to the case where different drivers are assigned different vehicles based on the distance driven per day, we incorporate a new decision variable s_i that defines the cutoff point such that drivers who travel less than s_i per day are assigned the vehicle defined by $\mathbf{x}_i$ and drivers who travel more than s_i per day are assigned the vehicle defined by $\mathbf{x}_{i+1}$. Extending this idea to multiple segments, the formulation for vehicle design and ordered allocation is given by

$$\begin{aligned} &\underset{\mathbf{x}_i, s_i \forall i \in \{1,\dots,n\}}{\text{minimize}} \sum_{i=1}^{n}\left(\int_{s_{i-1}}^{s_i} f_O(\mathbf{x}_i,s)\, f_S(s)\, ds\right) \\ &\text{subject to } \mathbf{g}(\mathbf{x}_i) \le \mathbf{0};\ \mathbf{h}(\mathbf{x}_i) = \mathbf{0};\ \forall i \in \{1,\dots,n\} \\ &\qquad\qquad s_i \ge s_{i-1};\ \ \forall i \in \{1,\dots,n\} \\ &\text{where } s_0 = 0;\ s_n = \infty \end{aligned} \tag{2}$$

Taking a two-vehicle-segment case as an example, the vehicle 1 segment contains vehicles that travel between $[0, s_1]$ miles per day; the vehicle 2 segment contains vehicles that travel between $[s_1, \infty]$ miles per day; and the optimal value of s_1 is determined together with the vectors of vehicle design variables $\mathbf{x}_1$ and $\mathbf{x}_2$ for vehicle 1 and vehicle 2.

2.1 Distribution of Vehicle Miles Travelled per Day

We use the 2009 National Household Transportation Survey (NHTS) data [5] to estimate the distribution of distance driven per day over the population of drivers. The survey collected data by interviewing 136,140 households across the U.S. on the mode of transportation, duration, distance and purpose of the trips taken on the survey day. We fit the weighted driving data[5] using the exponential distribution. The probability density function below represents the probability density function for vehicle miles traveled by drivers on the day surveyed:

$$f_{\mathrm{S}}\left(s\right)=\lambda e^{-\lambda s};\;\; s\geq 0 \tag{3}$$

The coefficient λ is 0.0296 estimated using the maximum likelihood method. Because we lack multiple days of data for each vehicle, we assume that a vehicle that travels *s* miles per day on the NHTS survey day will travel *s* miles every day. This assumption will produce optimistic results on the benefits of optimal allocation, since distance traveled varies over time for individual vehicles in practice.

2.2 Vehicle Performance Models

The vehicle performance evaluations are carried out using the Powertrain System Analysis Toolkit (PSAT) vehicle physical simulator developed by Argonne National Laboratory [11]. In our study the body, powertrain and vehicle parameters for all PHEV and HEV simulations are based on the 2004 Toyota Prius model that uses the split powertrain system with an Atkinson engine, a permanent magnet motor, and a nickel-metal hydride (NiMH) battery pack. To account for structural weight needed to carry heavy battery packs, we include an additional 1 kg of structural weight per 1 kg of battery and motor weight [12]. We created a comparable conventional vehicle (CV) model using a conventional powertrain and 4-cylinder engine to account for larger engine torque and power requirements, and the parameters that define the frontal area, drag coefficient and base weight are adjusted to match the Prius for fair comparison.

For the PHEV design, the Prius engine size is scaled by the peak power output from the base engine (57 kW) using a linear scaling algorithm. Similarly, the motor is scaled from the base motor (52 kW) linearly. Both the engine and motor weights are also scaled proportionally to the peak power. We use the Saft Li-ion battery module in the PSAT package for the PHEV energy storage device. Each cell in the module weighs 0.378 kg, with a modified specific energy of 100 Wh/kg and has a battery cell energy capacity of 21.6 Wh with a nominal output voltage of 3.6 volts. The weight of each 3-cell module is 1.42 kg after accounting for a packaging factor of 1.25. The battery size and capacity are scaled by specifying the number of cells in the battery pack. We assume an 800W base electrical hotel load on the PHEV, the HEV and the CV. To estimate the performance of a PHEV, we use the federal standard Urban Dynamometer Driving Schedule (UDDS) driving cycle [13] to calculate simulated electrical efficiency (miles/kWh) in CD-mode for PHEVs, and gasoline efficiency (mpg) in CS-mode for PHEVs as well as for HEVs and CVs.[6] We also perform a simulated performance test to calculate the time required to accelerate the vehicle from 0 to 60 miles per hour (mph) in the CD mode and in the CS mode.

Because the GHG emissions per mile associated with HEVs and CVs are independent of the number of miles driven per day, we take the HEV and CV to have fixed designs. The HEV is identical to the Prius model, which has a configuration of peak engine power 57 kW, motor power 52 kW, NiMH battery size 168 cells (1.3 kWh), fuel efficiency 60.1 miles per gallon, and 0-60 mph acceleration time 11.0 seconds. Similarly, our CV has an engine size 126 kW and fuel efficiency 29.5 miles per gallon, and 0-60 mph acceleration time 11.0 seconds. For the PHEVs, the design variables $\mathbf{x}$ consist of the engine scaling factor x_1, motor scaling factor x_2, battery pack scaling factor x_3, and battery energy swing x_4. We created a set of polynomial meta-model fits as functions of $\mathbf{x}$ for the PHEV using discrete simulation data points: (1) CD-mode electricity efficiency η_{E} (mile per kWh); (2) CS-mode gasoline efficiency η_{G} (mile per gallon); (3) CD-mode 0-60 mph acceleration time t_{CD} (second); (4) CS-mode 0-60 mph acceleration time t_{CS} (second); (5) CD-mode battery energy processed (charging and discharging) per mile μ_{CD} (kWh/mile); (6) CS-mode battery energy processed per mile μ_{CS} (kWh/mile); and (7) final SOC after completing multiple US06 aggressive driving cycles in CS mode u_{CS} (starting at the target SOC). Metamodels of η_{E} and η_{G} are used to calculate energy consumption; t_{CD} and t_{CS} are used to ensure comparison of equivalent-performance vehicles; μ_{CD} and μ_{CS} are usd to calculate battery degradation, and u_{CS} is used to ensure the engine is capable of providing average power needs in CS mode. We evaluated these output values using PSAT over a grid of values for the inputs x_1 = {30, 45, 60}/57, x_2 = {50, 70, 90, 110}/52, x_3 = {200, 400, 600, 800, 1000}/1000, and multivariate polynomial functions were fit to the data using least squares. The general form of the cubic fitting function f_{m3} is defined as (the subscript 3 indicates the PHEV case, which will be discussed later).

$$\begin{aligned}f_{m3}\left(\mathbf{x}\right)&=a_{m1}x_1^3+a_{m2}x_2^3+a_{m3}x_3^3+a_{m4}x_1^2+a_{m5}x_1x_2^2\\&+a_{m6}x_1^2x_3+a_{m7}x_1x_3^2+a_{m8}x_2^2x_3+a_{m9}x_2x_3^2+a_{m10}x_1x_2x_3\\&+a_{m11}x_1^2+a_{m12}x_2^2+a_{m13}x_3^2+a_{m14}x_1x_2+a_{m15}x_1x_3\\&+a_{m16}x_2x_3+a_{i17}x_1+a_{m18}x_2+a_{m19}x_3+a_{m20}\end{aligned} \tag{4}$$

where the a_m terms are the coefficients for function *m*. The polynomial fitting coefficients for η_{E}, η_{G}, t_{CD}, t_{CS}, μ_{CD}, μ_{CS} and u_{CS} are listed in Table A1 in Appendix.[7] The maximum

[5] We excluded data entries of publication transportation and also excluded drivers who traveled zero miles or more than 200 miles. We fit the distribution to the reported distance traveled on the survey day, and we assume that (1) the survey data calibrated with weightings are representative of the national population, and (2) the distance driven on the survey day is the same distance driven every day for that vehicle.

[6] Examination of alternative driving cycles and the correlation between driving cycle and driving distance is left for future work.

[7] We truncated the acceleration data points greater than 13.0 seconds to improve the metamodel fit, and fit μ_{CD}, μ_{CS} and u_{CS} using quadratic terms to avoid over-fitting.

metamodel error among the test points is 0.1 miles/kWh, 0.1 miles/gallon, 0.5 seconds, 0.02 kWh, and 0.5% for electrical efficiency, gasoline efficiency, acceleration time, energy processed, and final SOC, respectively.

2.3 Electric Travel and Battery Degradation

To calculate the objective function of GHG emissions, we first define the distance driven on electric power s_E and the distance driven on gasoline s_G as a function of the vehicle's AER s_{AER} and the total distance driven per day s. Assuming one charge per day, s_E and s_G are given by

$$s_E(\mathbf{x},s)=\begin{cases} s & \text{if } s\le s_{AER} \\ s_{AER}(\mathbf{x}) & \text{if } s>s_{AER}\end{cases}$$
$$s_G(\mathbf{x},s)=\begin{cases} 0 & \text{if } s\le s_{AER} \\ s-s_{AER}(\mathbf{x}) & \text{if } s>s_{AER}\end{cases} \tag{5}$$

For PHEVs, we assume that the battery is fully charged once each day. For HEVs and CVs, there is no electrical travel; thus HEV and CV can be seen as special cases with $s_{AER} = 0$, so that $s_E = 0$ and $s_G = s$. Assuming constant efficiency η_E (mile per kWh) in CD-mode, the AER of a PHEV can be calculated from the energy capacity per battery cell $\kappa = 0.0216$ kWh/cell, the (scaled) number of cells x_3, and the battery swing x_4:

$$s_{AER}(\mathbf{x})=\kappa(1000x_3)x_4\eta_E \tag{6}$$

We use the Peterson model [14] for estimating battery degradation and replacement. The model was constructed by cycling modern A123 $LiFePO_4$ cells under representative driving cycles (non-constant C-rate) and measuring capacity fade as a function of energy processed, including intermediate charging and discharging over the driving cycle. Results show relative energy capacity fade as a linear function of normalized energy processed while driving and while charging. The daily energy processed while driving w_{DRV} and charging w_{CHG} a PHEV can be expressed as (unit in kWh):

$$w_{DRV}(\mathbf{x},s)=\mu_{CD}s_E+\mu_{CS}s_G$$
$$w_{CHG}(\mathbf{x},s)=\frac{s_E}{\eta_E\eta_B} \tag{7}$$

where μ_{CD} and μ_{CS} are energy processed per mile (kWh/mile) in CD and CS mode, respectively, and η_B is battery charging efficiency 95% [14]. We assume that energy processed for daily charging is equal to net energy consumed in electrical travel per day. The relative energy capacity decrease can be calculated by the energy processed in driving and charging per cycle per cell per original cell energy capacity:

$$r_P(\mathbf{x},s)=\frac{\alpha_{DRV}w_{DRV}+\alpha_{CHG}w_{CHG}}{(1000x_3)\kappa} \tag{8}$$

where $\alpha_{DRV} = 3.46\times10^{-5}$ and $\alpha_{CHG} = 1.72\times10^{-5}$ are the coefficients for relative energy capacity fade. These coefficients are derived from the same data set described in [14].[8] If the battery end-of-life is defined as the point when the drop in relative energy capacity is r_{EOL}, the battery life θ_{BAT}, measured in days (or, equivalently, cycles), can be calculated as

$$\theta_{BAT}=\frac{r_{EOL}}{r_P}=\frac{(1000x_3)\kappa r_{EOL}}{\alpha_{DRV}(\mu_{CD}s_E+\mu_{CS}s_G)+\alpha_{CHG}s_E(\eta_E\eta_B)^{-1}} \tag{9}$$

The r_{EOL} criterion is defined at 20% [14] .

2.4 Objective and Constraint Functions

The operating (use phase) GHG emissions v_{OP} represents the average GHG emissions in kg CO_2 equivalent (kg-CO_2-eq) per day associated with the lifecycle of gasoline and electricity used to propel the vehicle:

$$v_{OP}(\mathbf{x},s)=\frac{s_E(\mathbf{x},s)}{\eta_E(\mathbf{x})}\frac{v_E}{\eta_C}+\frac{s_G(\mathbf{x},s)}{\eta_G(\mathbf{x})}v_G \tag{10}$$

where $\eta_C = 88\%$ for battery charging efficiency [15], $v_E = 0.752$ kg-CO_2-eq per kWh for electricity emissions[9], and $v_G = 11.34$ kg-CO_2-eq per gallon for gasoline lifecycle emissions. Total lifecycle GHG emissions further includes the GHGs associated with production of the vehicle and battery. The average total lifecycle GHG emissions per day $f_V(\mathbf{x}, s)$ is

$$f_V(\mathbf{x},s)=\left(\frac{s_E(\mathbf{x},s)}{\eta_E(\mathbf{x})}\frac{v_E}{\eta_C}+\frac{s_G(\mathbf{x},s)}{\eta_G(\mathbf{x})}v_G\right)+\left(\frac{v_{VEH}}{\theta_{VEH}(s)}\right)+\left(\frac{1000x_3\kappa v_{BAT}}{\theta_{BRPL}(\mathbf{x},s)}\right) \tag{11}$$

where $\theta_{VEH} = s_{LIFE}/s$ is the vehicle life in days, $s_{LIFE} = 150{,}000$ miles[10] is the vehicle life in miles, θ_{BRPL} is the battery replacement effective life (defined below), $v_{BAT} = 120$ kg-CO_2-eq per kWh for Li-ion battery and 230 kg-CO2-eq per kWh for NiMH battery is the lifecycle GHG emissions associated with battery production, $v_{VEH} = 8{,}500$ kg-CO_2-eq per vehicle is the lifecycle GHG emissions associated with vehicle production (excluding emissions from battery production) [4].

To compare comparable vehicles, we require that all vehicles meet a minimum acceleration constraint of 0-60 mph in less than 11 seconds. Because we have limited our scope to all-electric PHEVs, we require the acceleration constraint to be satisfied both in CD mode, using electric power alone, and in CS mode, where the gasoline engine is also used. The resulting constraints are $t_{CD}(\mathbf{x}) \le 11$s and $t_{CS}(\mathbf{x}) \le 11$s. Additionally, we require the gasoline engine to be large enough to provide average power for the vehicle in CS mode under an aggressive US06 driving cycle while maintaining the target SOC level in the battery. The resulting constraint is $u_{CS}(\mathbf{x}) \ge 32\%$. Finally, we impose simple bounds on the decision variables: $30/57 \le x_1 \le 60/57$, $50/52 \le x_2 \le 110/52$, $200/1000 \le x_3 \le 1000/1000$, $0 \le x_4$

[8] The regression in [14] focused on finding the degradation from energy arbitrage, but in this paper the data was assigned to categories to enable predictions about degradation due to driving and recharging.

[9] The lifecycle GHG emissions of electricity is estimated using the US national average electricity emission factor 0.69 kg-CO_2-eq/kWh [16] with 9% transmission loss [17].

[10] We assume that all vehicles must be replaced every 150,000 miles, which represents the U.S. average vehicle life [18]. This assumption may be unrealistic for vehicles driven very short or very long daily distances because other time-based factors also play a role in vehicle deterioration. However, these factors are only significant for regions of the objective function's integrand that are relatively insignificant to the integrated objective function, and they do not provide a significant source of error.

$\leq$ 0.8 to avoid metamodel extrapolation. Any active simple bounds would imply a modeling limitation rather than a physical optimum.

2.5 MINLP Reformulation

The resulting model formulation (Eq. (2)) involves integration, discrete decisions (vehicle type), and piecewise-smooth functions with derivative discontinuities due to AER and battery life. To solve the problem globally, we pose a factorable, algebraic nonconvex MINLP reformulation that can be solved using the BARON convexification-based branch-and-reduce algorithm [19]. First, the exponential distribution form for the NHTS data fit allows the integral in Eq. (2) to be simplified in terms of two algebraic formulae: the cumulative density function F_S:

$$\begin{aligned} F_S(s_i) &= \int_0^{s_i} f(s)ds = \int_0^{s_i} \lambda e^{-\lambda s} ds \\ &= \left[-e^{-\lambda s}\right]_0^{s_i} = 1 - e^{-\lambda s_i} \end{aligned} \tag{12}$$

and the partial expected value function F_E:

$$\begin{aligned} F_E(s_i) &= \int_0^{s_i} s f_S(s) ds = \int_0^{s_i} \lambda s e^{-\lambda s} ds \\ &= \left[-se^{-\lambda s}\right]_0^{s_i} + \int_0^{s_i} e^{-\lambda s} ds = \frac{1}{\lambda} - e^{-\lambda s_i}\left(s_i + \frac{1}{\lambda}\right) \end{aligned} \tag{13}$$

Thus the problem reduces to an algebraic formulation with discrete vehicle-type decisions and piecewise-smooth functions. We next introduce four sets of binary variables to convert the problem to a twice-differentiable MINLP. The first binary variable set t_{il} identifies the vehicle type $l \in \{1,2,..,L\}$ for each segment i, where $t_{il} \in \{0,1\}$ $\forall i,l$ and $\Sigma_l t_{il} = 1$ $\forall i$. Here we consider three vehicle types $l \in \{1,2,3\}$ for CV, HEV and PHEV, respectively, and write the objective function as a binary-weighted function $\sum_l (t_l)(f_l(\mathrm{x}_l, s))$.

The second binary variable set $z_{ij} \in \{0,1\}$ $\forall i,j$ handles one of the derivative discontinuities by identifying in which of three regions $j \in \{1,2,3\}$ on the s-axis each segment i is located, relative to s_{AER} ($\Sigma_j z_{ij} = 1$ $\forall i$).

(1) In region 1, $s_{\mathrm{AER}} \leq s_i \Rightarrow (z_{i1})(s_{\mathrm{AER}}(\mathrm{x}_i) - s_{i-1}) \leq 0$;
(2) in region 2, $s_{i-1} \leq s_{\mathrm{AER}} \leq s_i \Rightarrow (z_{i2})(s_{i-1} - s_{\mathrm{AER}}(\mathbf{x}_i)) \leq 0$ and $(z_{i2})(s_{\mathrm{AER}}(\mathbf{x}_i) - s_i) \leq 0$;
(3) in region 3, $s_{\mathrm{AER}} \geq s_i \Rightarrow (z_{i3})(s_i - s_{\mathrm{AER}}(\mathrm{x}_i)) \leq 0$.

The population-weighted operation GHG emissions are

$$\begin{aligned} F_{i\mathrm{OG}} &= \int_{s_{i-1}}^{s_i} \left(\frac{s_E(\mathbf{x},s)}{\eta_E(\mathbf{x})}\frac{v_E}{\eta_C} + \frac{s_G(\mathbf{x},s)}{\eta_G(\mathbf{x})} v_G \right) f_S(s) ds \\ &= \begin{cases} \text{if } s_{\mathrm{AER}} \leq s_{i-1}: & \int_{s_{i-1}}^{s_i} \frac{v_E}{\eta_E\eta_C} s_E + \frac{v_G}{\eta_G} s_G \lambda e^{-\lambda s} ds \\ \text{if } s_{i-1} \leq s_{\mathrm{AER}} \leq s_i: & \\ \int_{s_{i-1}}^{s_{\mathrm{AER}}} \frac{v_E}{\eta_E\eta_C} s_E \lambda e^{-\lambda s} ds + \int_{s_{\mathrm{AER}}}^{s_i}\left(\frac{v_E}{\eta_E\eta_C} s_E + \frac{v_G}{\eta_G} s_G\right)\lambda e^{-\lambda s} ds & \\ \text{if } s_i \leq s_{\mathrm{AER}}: & \int_{s_{i-1}}^{s_i} \frac{v_E}{\eta_E\eta_C} s_E \lambda e^{-\lambda s} ds \end{cases} \end{aligned} \tag{14}$$

Applying Eq. (12) and (13), the above integral can be expressed as the sum of three analytical functions:

$$\begin{aligned} & F_{i\mathrm{OG}} = \sum_{j=1}^{3} z_{ij} F_{i\mathrm{OG}j}\left(\mathbf{x}_{il}, s_{i-1}, s_i\right) \\ & j=1,\ s_{\mathrm{AER}} \leq s_{i-1}: \\ & \quad F_{i\mathrm{OG1}} = \frac{v_G}{\eta_G}\left(F_E(s_i) - F_E(s_{i-1})\right) \\ & \qquad + s_{\mathrm{AER}}\left(\frac{v_E}{\eta_E\eta_C} - \frac{v_G}{\eta_G}\right)\left(F_S(s_i) - F_S(s_{i-1})\right) \\ & j=2,\ s_{i-1} \leq s_{\mathrm{AER}} \leq s_i: \\ & \quad F_{i\mathrm{OG2}} = \frac{v_E}{\eta_E\eta_C}\left(F_E(s_{\mathrm{AER}}) - F_E(s_{i-1})\right) + \frac{v_G}{\eta_G}\left(F_E(s_i) - F_E(s_{\mathrm{AER}})\right) \\ & \qquad + s_{\mathrm{AER}}\left(\frac{v_E}{\eta_E\eta_C} - \frac{v_G}{\eta_G}\right)\left(F_S(s_i) - F_S(s_{\mathrm{AER}})\right) \\ & j=3,\ s_i \leq s_{\mathrm{AER}}: \\ & \quad F_{i\mathrm{OG3}} = \frac{v_E}{\eta_E\eta_C}\left(F_E(s_i) - F_E(s_{i-1})\right) \end{aligned} \tag{15}$$

The third binary variable set q_{io} $o \in \{1,2,3\}$ and $\Sigma_o q_{io} = 1$ $\forall i$ identifies the relative conditions between battery life θ_{BAT} and vehicle life θ_{VEH}. Here we define the battery life in vehicle mileage travelled (VMT) as $s_{\mathrm{BAT}} = s\theta_{\mathrm{BAT}}$, assuming one charge per day. The estimated battery life s_{BAT} using the Peterson degradation model is a non-decreasing function of s:

$$\begin{aligned} & s_{\mathrm{BAT}}(\mathbf{x}, s) = s\theta_{\mathrm{BAT}} \\ & = \frac{(1000x_3)\kappa r_{\mathrm{EOL}} s}{\alpha_{\mathrm{DRV}}\left(\mu_{\mathrm{CD}} s_E + \mu_{\mathrm{CS}} s_G\right) + \alpha_{\mathrm{CHG}} s_E \left(\eta_E\eta_B\right)^{-1}} \\ & = \begin{cases} \text{if } s \leq s_{\mathrm{AER}}: \ \dfrac{(1000x_3)\kappa r_{\mathrm{EOL}}}{\alpha_{\mathrm{DRV}}\mu_{\mathrm{CD}} + \alpha_{\mathrm{CHG}}\left(\eta_E\eta_B\right)^{-1}} = s_{\mathrm{BAT}}^0 \\ \text{if } s > s_{\mathrm{AER}}: \\ \dfrac{(1000x_3)\kappa r_{\mathrm{EOL}}}{s^{-1}s_{\mathrm{AER}}\left(\alpha_{\mathrm{DRV}}\left(\mu_{\mathrm{CD}} - \mu_{\mathrm{CS}}\right) + \alpha_{\mathrm{CHG}}\left(\eta_E\eta_B\right)^{-1}\right) + \alpha_{\mathrm{DRV}}\mu_{\mathrm{CS}}} \\ \text{if } s \to \infty: \ \dfrac{(1000x_3)\kappa r_{\mathrm{EOL}}}{\alpha_{\mathrm{DRV}}\mu_{\mathrm{CS}}} = s_{\mathrm{BAT}}^{\infty} \end{cases} \end{aligned} \tag{16}$$

The expression for $s \rightarrow \infty$ is simplified from the conditional expression for $s > s_{\mathrm{AER}}$ by imposing $s^{-1} \rightarrow 0$. The function s_{BAT} has two unique characteristics. First, the function value is a constant when $s \leq s_{\mathrm{AER}}$. Second, when $s \geq s_{\mathrm{AER}}$, s_{BAT} is a monotonically increasing function and asymptotically approaches the life of the battery on energy processed in CS mode, which is the constant value under $s \rightarrow \infty$ condition. Because of the unique features in s_{BAT}, we are able to identify four possible relations between s_{BAT} and vehicle life s_{LIFE}:

(a) battery life $s_{\mathrm{BAT}}(\mathbf{x}, s)$ is less than vehicle life s_{LIFE} for all s;
(b) s_{BAT} curve and s_{LIFE} curve has one intersection point s_T, where $s_{\mathrm{LIFE}} > s_{\mathrm{BAT}}$ for $0 \leq s \leq s_T$ and $s_{\mathrm{BAT}} > s_{\mathrm{LIFE}}$ for $s \geq s_T$;
(c) the flat region of s_{BAT} overlaps with s_{LIFE} ($s_{\mathrm{BAT}} = s_{\mathrm{LIFE}}$) for $0 \leq s \leq s_{\mathrm{AER}}$, and $s_{\mathrm{BAT}} > s_{\mathrm{LIFE}}$ for $s \geq s_T$; and
(d) s_{BAT} is greater than vehicle life s_{LIFE} for all s.

The four conditions are illustrated in Figure 3.

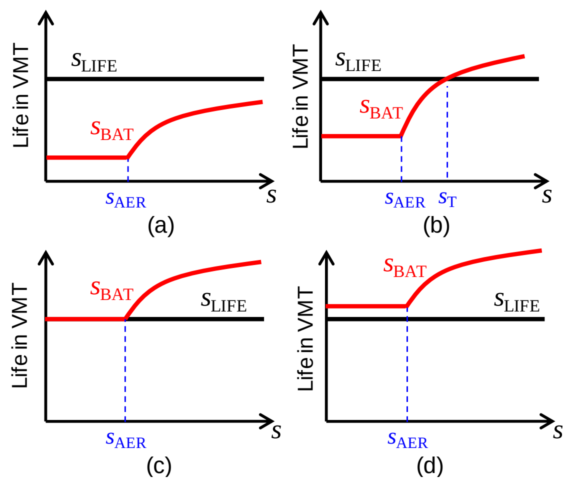

Figure 3. Four conditions for the battery and vehicle VMT curves

Condition (a) occurs when the following inequality is valid:

$$s_{\mathrm{BAT}}^{\infty} \le s_{\mathrm{LIFE}} \tag{17}$$

For condition (b), an analytical expression for s_{T} is available by solving $s_{\mathrm{LIFE}}=s_{\mathrm{BAT}}(\mathbf{x},s_{\mathrm{T}})$:

$$s_{\mathrm{T}}(\mathbf{x})=\frac{s_{\mathrm{LIFE}}s_{\mathrm{AER}}\left(\alpha_{\mathrm{DRV}}\left(\mu_{\mathrm{CD}}-\mu_{\mathrm{CS}}\right)+\alpha_{\mathrm{CHG}}\left(\eta_{\mathrm{E}}\eta_{\mathrm{B}}\right)^{-1}\right)}{r_{\mathrm{EOL}}\kappa\left(1000x_3\right)-\alpha_{\mathrm{DRV}}\mu_{\mathrm{CS}}s_{\mathrm{LIFE}}} \tag{18}$$

Condition (c) and (d) occur when the following inequality is valid:

$$s_{\mathrm{BAT}}^{0} \ge s_{\mathrm{LIFE}} \tag{19}$$

The battery replacement effective life θ_{BRPL} under the buy-lease scenario is determined by min(θ_{VEH}, θ_{BAT}). Therefore, three discrete cases are identified:

(1) In case 1 (o=1), $s^{\infty}{}_{\mathrm{BAT}} \le s_{\mathrm{LIFE}}$ ($\theta_{\mathrm{BAT}} < \theta_{\mathrm{VEH}}$) $\forall s \Rightarrow (q_{i1})(\theta_{\mathrm{BAT}}(s\Rightarrow\infty)-\theta_{\mathrm{VEH}}) \le 0$ and $\theta_{\mathrm{BRPL}} = \theta_{\mathrm{BAT}}$;

(2) for case 2 (o=2), θ_{BAT} intersects θ_{VEH} at a point $s_{\mathrm{T}} \Rightarrow (q_{i2})(\theta_{\mathrm{VEH}}-\theta_{\mathrm{BAT}}(s\Rightarrow\infty)) \le 0$ and $(q_{i2})(\theta_{\mathrm{BAT}}(s=0)-\theta_{\mathrm{VEH}}) \le 0$, so $\theta_{\mathrm{BRPL}} = \theta_{\mathrm{BAT}}$ for $s \le s_{\mathrm{T}}$, $\theta_{\mathrm{BRPL}} = \theta_{\mathrm{VEH}}$ for $s \ge s_{\mathrm{T}}$; and

(3) for case 3 (o=3), $s^{0}{}_{\mathrm{BAT}} \ge s_{\mathrm{LIFE}}$ ($\theta_{\mathrm{BAT}} \ge \theta_{\mathrm{VEH}}$) $\forall s \Rightarrow (q_{i3})(\theta_{\mathrm{VEH}}-\theta_{\mathrm{BAT}}(s=0)) \le 0$ and $\theta_{\mathrm{BRPL}} = \theta_{\mathrm{VEH}}$.

The fourth binary variable set y_{ik} identifies in which region s_{T} lies when q_{i2} = 1 (o=2). The three conditions $k\in\{1,2,3\}$ on the binary variable set y_{ik} are:

(1) In region 1 (k=1), $s_{\mathrm{T}}(\mathbf{x}_i) \le s_{i-1} \Rightarrow (q_{i2})(y_{i1})(s_{\mathrm{T}}(\mathbf{x}_i)-s_{i-1}) < 0$;

(2) in region 2 (k=2), $s_{i-1} \le s_{\mathrm{T}} \le s_i \Rightarrow (q_{i2})(y_{i2})(s_{i-1}-s_{\mathrm{T}}(\mathbf{x}_i)) \le 0$ and $(q_{i2})(y_{i2})(s_{\mathrm{T}}(\mathbf{x}_i)-s_i) \le 0$; and

(3) in region 3 (k=3), $s_{\mathrm{T}}(\mathbf{x}_i) \ge s_i \Rightarrow (q_{i2})(y_{i3})(s_i-s_{\mathrm{T}}(\mathbf{x}_i)) \le 0$.

The combinations of j, k and o result in 27 cases. For each segment i, for each of the cases $j\in\{1,2,3\}$ $k\in\{1,2,3\}$ $o\in\{1,2,3\}$, the integral in Eq. (2) reduces to a twice-differentiable closed form factorable algebraic expression $F_{ijko}(\mathbf{x}_{il}, s_{i-1}, s_i)$. Table 1 presents the summary of the discrete conditions with corresponding θ_{BRPL} and the components in the total cost function. Among the o=2 cases, there are three infeasible cases because the value of s_{T} should be greater than s_{AER} when an s_{T} point exists. The analytical expressions of battery GHG emission function F_{BG} for all discrete cases are listed in follows:

Case (1a): $\theta_{\mathrm{BRPL}} = \theta_{\mathrm{BAT}}$ and $s_{\mathrm{AER}} \le s_{i-1}$

$$\begin{aligned}F_{\mathrm{BG1a}}=\frac{v_{\mathrm{BAT}}}{r_{\mathrm{EOL}}}\Big[&\alpha_{\mathrm{DRV}}w_{\mathrm{CS}}\left(F_{\mathrm{E}}(s_i)-F_{\mathrm{E}}(s_{i-1})\right)\\&+s_{\mathrm{AER}}\left(\alpha_{\mathrm{DRV}}w_{\mathrm{CD}}+\alpha_{\mathrm{CHG}}\left(\eta_{\mathrm{E}}\eta_{\mathrm{B}}\right)^{-1}-\alpha_{\mathrm{DRV}}w_{\mathrm{CS}}\right)\\&\left(F_{\mathrm{S}}(s_i)-F_{\mathrm{S}}(s_{i-1})\right)\Big]\end{aligned} \tag{20}$$

Case (1b): $\theta_{\mathrm{BRPL}} = \theta_{\mathrm{BAT}}$ and $s_{i-1} \le s_{\mathrm{AER}} \le s_i$

$$\begin{aligned}&F_{\mathrm{BG1b}}\\&=\frac{v_{\mathrm{BAT}}}{r_{\mathrm{EOL}}}\Big[\left(\alpha_{\mathrm{DRV}}\mu_{\mathrm{CD}}+\alpha_{\mathrm{CHG}}\left(\eta_{\mathrm{E}}\eta_{\mathrm{B}}\right)^{-1}\right)\left(F_{\mathrm{E}}(s_{\mathrm{AER}})-F_{\mathrm{E}}(s_{i-1})\right)\\&\quad+\alpha_{\mathrm{DRV}}\mu_{\mathrm{CS}}\left(F_{\mathrm{E}}(s_i)-F_{\mathrm{E}}(s_{\mathrm{AER}})\right)\\&\quad+s_{\mathrm{AER}}\left(\alpha_{\mathrm{DRV}}\mu_{\mathrm{CD}}+\alpha_{\mathrm{CHG}}\left(\eta_{\mathrm{E}}\eta_{\mathrm{B}}\right)^{-1}-\alpha_{\mathrm{DRV}}\mu_{\mathrm{CS}}\right)\\&\quad\left(F_{\mathrm{S}}(s_i)-F_{\mathrm{S}}(s_{\mathrm{AER}})\right)\Big]\end{aligned} \tag{21}$$

Case (1c): $\theta_{\mathrm{BRPL}} = \theta_{\mathrm{BAT}}$ and $s_i \le s_{\mathrm{AER}}$

$$F_{\mathrm{BG1c}}=\frac{v_{\mathrm{BAT}}}{r_{\mathrm{EOL}}}\left(\alpha_{\mathrm{DRV}}\mu_{\mathrm{CD}}+\alpha_{\mathrm{CHG}}\eta_{\mathrm{E}}^{-1}\right)\left(F_{\mathrm{E}}(s_i)-F_{\mathrm{E}}(s_{i-1})\right) \tag{22}$$

Case (2a): $\theta_{\mathrm{BRPL}} = \{\theta_{\mathrm{BAT}}, \theta_{\mathrm{VEH}}\}$ and $s_{\mathrm{AER}} \le s_{i-1}$

$$\begin{aligned}F_{\mathrm{BG2a}}=\frac{v_{\mathrm{BAT}}}{r_{\mathrm{EOL}}}\Big[&\alpha_{\mathrm{DRV}}\mu_{\mathrm{CS}}\left(F_{\mathrm{E}}(s_{\mathrm{T}})-F_{\mathrm{E}}(s_{i-1})\right)\\&+s_{\mathrm{AER}}\left(\alpha_{\mathrm{DRV}}\mu_{\mathrm{CD}}+\alpha_{\mathrm{CHG}}\left(\eta_{\mathrm{E}}\eta_{\mathrm{B}}\right)^{-1}-\alpha_{\mathrm{DRV}}\mu_{\mathrm{CS}}\right)\\&\left(F_{\mathrm{S}}(s_{\mathrm{T}})-F_{\mathrm{S}}(s_{i-1})\right)\Big]\\&+\frac{1000x_3\kappa v_{\mathrm{BAT}}}{s_{\mathrm{LIFE}}}\left(F_{\mathrm{E}}(s_i)-F_{\mathrm{E}}(s_{\mathrm{T}})\right)\end{aligned} \tag{23}$$

Case (2b): $\theta_{\mathrm{BRPL}} = \{\theta_{\mathrm{BAT}}, \theta_{\mathrm{VEH}}\}$ and $s_{i-1} \le s_{\mathrm{AER}} \le s_i$

$$\begin{aligned}&F_{\mathrm{BG2b}}\\&=\frac{v_{\mathrm{BAT}}}{r_{\mathrm{EOL}}}\Big[\left(\alpha_{\mathrm{DRV}}\mu_{\mathrm{CD}}+\alpha_{\mathrm{CHG}}\left(\eta_{\mathrm{E}}\eta_{\mathrm{B}}\right)^{-1}\right)\left(F_{\mathrm{E}}(s_{\mathrm{AER}})-F_{\mathrm{E}}(s_{i-1})\right)\\&\quad+\alpha_{\mathrm{DRV}}\mu_{\mathrm{CS}}\left(F_{\mathrm{E}}(s_{\mathrm{T}})-F_{\mathrm{E}}(s_{\mathrm{AER}})\right)\\&\quad+s_{\mathrm{AER}}\left(\alpha_{\mathrm{DRV}}\mu_{\mathrm{CD}}+\alpha_{\mathrm{CHG}}\left(\eta_{\mathrm{E}}\eta_{\mathrm{B}}\right)^{-1}-\alpha_{\mathrm{DRV}}\mu_{\mathrm{CS}}\right)\\&\quad\left(F_{\mathrm{S}}(s_{\mathrm{T}})-F_{\mathrm{S}}(s_{\mathrm{AER}})\right)\Big]\\&\quad+\frac{1000x_3\kappa v_{\mathrm{BAT}}}{s_{\mathrm{LIFE}}}\left(F_{\mathrm{E}}(s_i)-F_{\mathrm{E}}(s_{\mathrm{T}})\right)\end{aligned} \tag{24}$$

Case (3): $\theta_{\mathrm{BRPL}}=\theta_{\mathrm{VEH}}$

$$F_{\mathrm{BG3}}=\frac{1000x_3\kappa v_{\mathrm{BAT}}}{s_{\mathrm{LIFE}}}\left(F_{\mathrm{E}}(s_i)-F_{\mathrm{E}}(s_{i-1})\right) \tag{25}$$

Table 1. Discrete conditions for estimating total lifecycle emissions on the AER and battery life

o		*J*		*k*		θ_{BRPL}	Total GHG function F_{ijko}
		1	$s_{\text{AER}} \le s_{i\text{-}1}$				F_{i1k1}=v_{VEH}+F_{OG1}+F_{BG1a}
1	$s_{\text{BAT}}^{\infty} \le s_{\text{LIFE}}$	2	$s_{i\text{-}1} \le s_{\text{AER}} \le s_i$			θ_{BAT}	F_{i2k1}=v_{VEH}+F_{OG2}+F_{BG1b}
		3	$s_i \le s_{\text{AER}}$				F_{i3k1}=v_{VEH}+F_{OG3}+F_{BG1c}
				1	$s_{\text{T}} \le s_{i\text{-}1}$	θ_{VEH}	F_{i112}=v_{VEH}+F_{OG1}+F_{BG3}
		1	$s_{\text{AER}} \le s_{i\text{-}1}$	2	$s_{i\text{-}1} \le s_{\text{T}} \le s_i$	$\{\theta_{\text{BAT}}, \theta_{\text{VEH}}\}$	F_{i122}=v_{VEH}+F_{OG1}+F_{BG2a}
				3	$s_i \le s_{\text{T}}$	θ_{BAT}	F_{i132}=v_{VEH}+F_{OG1}+F_{BG1a}
				1	$s_{\text{T}} \le s_{i\text{-}1}$	Infeasible	
2	$s_{\text{BAT}}^{0} \le s_{\text{LIFE}} \le s_{\text{BAT}}^{\infty}$	2	$s_{i\text{-}1} \le s_{\text{AER}} \le s_i$	2	$s_{i\text{-}1} \le s_{\text{T}} \le s_i$	$\{\theta_{\text{BAT}}, \theta_{\text{VEH}}\}$	F_{i222}=v_{VEH}+F_{OG2}+F_{BG2b}
				3	$s_i \le s_{\text{T}}$	θ_{BAT}	F_{i232}=v_{VEH}+F_{OG2}+F_{BG1b}
				1	$s_{\text{T}} \le s_{i\text{-}1}$	Infeasible	
		3	$s_i \le s_{\text{AER}}$	2	$s_{i\text{-}1} \le s_{\text{T}} \le s_i$	Infeasible	
				3	$s_i \le s_{\text{T}}$	θ_{BAT}	F_{i332}=v_{VEH}+F_{OG3}+F_{BG1c}
		1	$s_{\text{AER}} \le s_{i\text{-}1}$				F_{i1k3}=v_{VEH}+F_{OG1}+F_{BG3}
3	$s_{\text{BAT}}^{0} \ge s_{\text{LIFE}}$	2	$s_{i\text{-}1} \le s_{\text{AER}} \le s_i$			θ_{VEH}	F_{i2k3}=v_{VEH}+F_{OG2}+F_{BG3}
		3	$s_i \le s_{\text{AER}}$				F_{i3k3}=v_{VEH}+F_{OG3}+F_{BG3}

The complete MINLP formulation is

$$\begin{aligned}
&\underset{\substack{\mathbf{x}_{il}, t_{il}, z_{ij}, y_{ik}, q_{io}, s_i \\ \forall i \in \{1,\dots,n\} \\ \forall l, j, k, o \in \{1,2,3\}}}{\text{minimize}} \quad \sum_{i=0}^{n}\sum_{l=1}^{3}\sum_{j=1}^{3}\sum_{k=1}^{3}\sum_{o=1}^{3} t_{il} z_{ij} y_{ik} q_{io} F_{ijko}\left(\mathbf{x}_{il}, s_{i-1}, s_i\right) \\
&\text{subject to } \mathbf{x}_l^{\text{LB}} \le \mathbf{x}_{il} \le \mathbf{x}_l^{\text{UB}};\ t_{\text{CD}} \le 11;\ t_{\text{CS}} \le 11;\ u_{\text{CS}} \ge 32\%; \\
&\sum\nolimits_{l=1}^{3} t_{il} = 1; \quad \sum\nolimits_{j=1}^{3} z_{ij} = 1; \quad \sum\nolimits_{k=1}^{3} y_{ik} = 1; \quad \sum\nolimits_{o=1}^{3} q_{io} = 1; \\
&s_{i-1} \le s_i; \\
&\left(z_{i1}\right)\left(s_{\text{AER}} - s_{i-1}\right) \le 0; \qquad \left(z_{i2}\right)\left(s_{i-1} - s_{\text{AER}}\right) \le 0; \\
&\left(z_{i2}\right)\left(s_{\text{AER}} - s_i\right) \le 0; \qquad \left(z_{i3}\right)\left(s_i - s_{\text{AER}}\right) \le 0; \\
&\left(q_{i1}\right)\left(s_{\text{BAT}}^{\infty} - s_{\text{LIFE}}\right) \le 0; \qquad \left(q_{i2}\right)\left(s_{\text{BAT}}^{0} - s_{\text{LIFE}}\right) \le 0; \\
&\left(q_{i2}\right)\left(s_{\text{LIFE}} - s_{\text{BAT}}^{\infty}\right) \le 0; \qquad \left(q_{i3}\right)\left(s_{\text{LIFE}} - s_{\text{BAT}}^{0}\right) \le 0; \\
&\left(q_{i2}\right)\left(y_{i1}\right)\left(s_{\text{T}} - s_{i-1}\right) \le 0; \quad \left(q_{i2}\right)\left(y_{i2}\right)\left(s_{i-1} - s_{\text{T}}\right) \le 0; \\
&\left(q_{i2}\right)\left(y_{i2}\right)\left(s_{\text{T}} - s_i\right) \le 0; \quad \left(q_{i2}\right)\left(y_{i3}\right)\left(s_i - s_{\text{T}}\right) \le 0; \\
&t_{il}, z_{ij}, y_{ik}, q_{io} \in \{0,1\}; \quad s_i \in \mathbb{R}; \quad \mathbf{x}_{il} \in \mathbb{R}^{p_l}; \\
&\forall i \in \{1,\dots,n\}; \quad \forall l, j, k, o \in \{1,2,3\} \\
&\text{where } s_0 = 0;\ s_n = \infty;\ s_{\text{AER}} = 10^3 t_{i3} \kappa x_3 x_4 \eta_{\text{E}}; \\
&s_{\text{BAT}}^{0} = \frac{10^3 x_3 \kappa r_{\text{EOL}}}{\alpha_{\text{DRV}} \mu_{\text{CD}} + \alpha_{\text{CHG}} \eta_{\text{E}}^{-1}}; \quad s_{\text{BAT}}^{\infty} = \frac{10^3 x_3 \kappa r_{\text{EOL}}}{\alpha_{\text{DRV}} \mu_{\text{CS}}}; \\
&s_{\text{T}} = \frac{s_{\text{LIFE}} s_{\text{AER}} \left(\alpha_{\text{DRV}}\left(\mu_{\text{CD}} - \mu_{\text{CS}}\right) + \alpha_{\text{CHG}} \eta_{\text{E}}^{-1}\right)}{10^3 x_3 \kappa r_{\text{EOL}} - \alpha_{\text{DRV}} \mu_{\text{CS}} s_{\text{LIFE}}} \\
&\eta_{\text{E}i} = \sum\nolimits_l t_{il} f_{1l}\left(\mathbf{x}_{il}\right);\ \eta_{\text{G}i} = \sum\nolimits_l t_{il} f_{2l}\left(\mathbf{x}_{il}\right); \\
&t_{\text{CD}i} = \sum\nolimits_l t_{il} f_{3l}\left(\mathbf{x}_{il}\right);\ t_{\text{CS}i} = \sum\nolimits_l t_{il} f_{4l}\left(\mathbf{x}_{il}\right); \\
&\mu_{\text{CD}i} = \sum\nolimits_l t_{il} f_{5l}\left(\mathbf{x}_{il}\right);\ \mu_{\text{CS}i} = \sum\nolimits_l t_{il} f_{6l}\left(\mathbf{x}_{il}\right); \\
&u_{\text{CS}i} = \sum\nolimits_l t_{il} f_{7l}\left(\mathbf{x}_{il}\right); \\
&F_{ijko}\left(\mathbf{x}_{il}, s_{i-1}, s_i\right) = \int_{s_{i-1}}^{s_i} f_{\text{O}}\left(\mathbf{x}_i, s\right) f_{\text{S}}\left(s\right) ds
\end{aligned} \tag{26}$$

where the expression for F_{ijko} reduces to a twice-differentiable algebraic expression in each case, $f_{11} = f_{12} = 0$, f_{21} = 29.5 mpg (CV), f_{22} = 60.1 mpg (HEV), $f_{31} = f_{32} = 0$, $f_{41} = f_{42}$ = 11 sec, $f_{51} = f_{52} = f_{61} = f_{62} = 0$, $f_{71} = f_{72} = 1$, and $f_{m3}(\mathbf{x}_{il})$ are defined in Eq. (4) for PHEVs (l=3 and t_{i3}=1) with coefficients listed in Table A1.

Here we summarize the primary modeling assumptions of this optimization framework: (1) Vehicles are designed and allocated to drivers based on VMT to minimize life cycle GHG emissions; (2) Each driver has a constant daily driving distance over the vehicle life; (3) The US NHTS weighted driving data are described using the exponential distribution function; (4) Vehicle performances are measured using EPA UDDS driving cycle simulation, and PHEV is assumed one full charge per day; (5) Lifecycle GHG emissions assume the average US grid mixture.

3. RESULTS AND DISCUSSION

We consider three driver segment scenarios, n=1, 2 and 3, and solve the MINLP model (Eq. (26)) using GAMS/BARON solver to obtain global solutions. The optimal vehicle type, design and allocation ranges for each case are summarized in Table 2. The first two data columns show the performance values of CV and HEV. We plot the functional values at the optimal solution $\mathbf{x}^*$ in Figure 4. The plots in the upper row show the lifecycle GHG emissions per mile $f_{\text{O}}(\mathbf{x}^*,s)/s$, and the plots in the lower row show the population-weighted lifecycle GHG emissions per day $f_{\text{O}}(\mathbf{x}^*,s)\cdot f_{\text{S}}(s)$. The area under the population-weighted curve is the net lifecycle GHG emissions per person per day in the United States.

Table 2. Solutions of minimum lifecycle GHGs with three driver segment scenarios

Driver segment scenario	Single segment			Two segments		Three segments		
	CV	HEV	PHEV	PHEV	PHEV	PHEV	PHEV	PHEV
Allocation (miles)	0-200	0-200	0-200	0-87	87-200	0-33	33-83	83-200
AER (miles)	−	−	36	40	25	29	46	25
Engine power (kW)	126	57	46	47	43	44	49	43
Motor power (kW)	−	52	70	71	73	71	72	73
Battery cells	−	168	396	435	269	316	512	274
Battery design swing	−	−	0.8†	0.8†	0.8†	0.8†	0.8†	0.8†
Battery capacity (kWh)	−	1.3	8.6	9.4	5.8	6.8	11.0	5.9
CD-mode eff. (miles/kWh)	−	−	5.30	5.29	5.35	5.33	5.25	5.34
CS-mode eff. (mpg)	29.5	60.1	60.2	60.0	60.7	60.5	59.6	60.7
CD-mode acceleration (sec)	−	−	11.0	11.0	11.0	11.0	11.0	11.0
CS-mode acceleration (sec)	11.0	11.0	9.3	9.1	10.3	9.8	8.9	10.2
Final SOC	−	−	0.32	0.32	0.32	0.32	0.32	0.32
GHG emissions (kg-eq-CO_2 per person-day)	14.6	8.2	7.78	7.77		7.75		
Reduction % from CV only	−	−43.8%	−46.7%	−46.8%		−46.9%		

†Variable limited by model boundary

For the single-segment case, we found that a PHEV36 has the lowest lifecycle GHG emissions. GHG emissions from the HEV scenario are about 44% lower than the CV scenario, and GHGs from the PHEVs scenarios are 5-6% lower than HEVs. For the two-segment case, the optimal solution is to allocate a PHEV40 to drivers who can charge every 87 miles or less (92% of drivers and 74% of VMT per day) and allocate a smaller-range PHEV25 to drivers who charge less frequently. This optimal allocation of two vehicles reduces daily GHG emissions by only an additional 0.1% compared to allocating all drivers a PHEV36. The solution of three-segment case similarly produces very slight additional GHG reduction, implying that a single segment is able to provide a practical solution for our evaluation of PHEV environmental performances. A significant reduction in GHG emissions is achieved by allocating PHEVs to drivers rather than HEVs or CVs, and there is only a marginal additional gain from optimal allocation in the two- and three-segment cases.

In the plots of the two-segment case (Figure 4(b) and (e)), there are two intersection points between the two PHEV GHG curves, and the optimal single cutoff point is located at the first intersection. Although the PHEV40 GHG curve surpasses the PHEV25 after 87 miles, the difference between two is almost indistinguishable, and the portion of the population driving greater than 87 miles/day is small. Assigning all drivers high-AER PHEVs can significantly reduce petroleum consumption, but this is not necessarily the best solution for minimizing GHGs because reducing the number of unnecessary batteries in these vehicles reduces the emissions associated with battery production as well as the emissions associated with reduced vehicle efficiency caused by carrying heavy batteries. While the largest group of vehicles travel short distances each day, the majority of the GHG emissions are produced by those vehicles that travel between about 25-45 miles/day.

We further tested the single segment case with low carbon electricity scenario (high portion of renewable energy sources) 218 kg-CO_2-eq/kWh in the grid mix [4]. The optimal solution shows an optimal large-capacity PHEV87 (upper bound) is best to reduce the average GHG emissions to 4.53 kg-CO_2-eq per person per day, and the reduction percentages from CV and HEV are 69% and 45%, respectively. This result implies grid decarbonization is needed in order for large capacity PHEVs to have significantly superior GHG performance than HEVs. This finding is consistent with prior studies [4, 12].

To compare the solution performance of the randomized multi-start method with global solutions, we use 1000 random starting points uniformly distributed in the design variable domain with the Matlab SQP NLP solver *fmincon* to find the minimum GHG solutions. The integrals in Eq. (1) and Eq. (2) are approximated by trapezoidal numerical integration, and the vehicle types for the two-segment and three-segment cases are preselected as PHEV-PHEV and PHEV-PHEV-PHEV, respectively. The solution quality is evaluated using relative error $|F-F^*|/F^*$, where F is the optimal objective value found by local solver with each multi-start and F^* is the global solution. The results are presented in Figure 5. All multi-start points reached feasible optimal solutions. For the single-segment model, the multi-start method performs very well, and all multi-start solutions reached the global optimum. For the two-segment case, 59% of the multi-start solutions reach the global optimum (within 10^{-6}). For the three-segment case, the ratio of finding the global solution decreases to 18%. Using different NLP solvers may affect the percentages, but the results show that when the numbers of driver segments and design variables increase, the probability of random starting points reaching global solution decreases significantly. In this case, local minima are all within 1% of the global minimum.

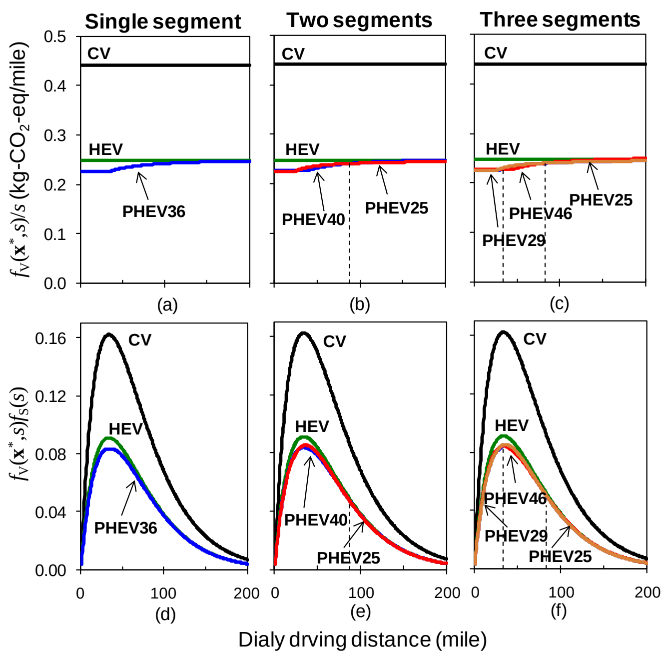

Figure 4. Optimal PHEV design and allocations for minimum lifecycle GHG emissions

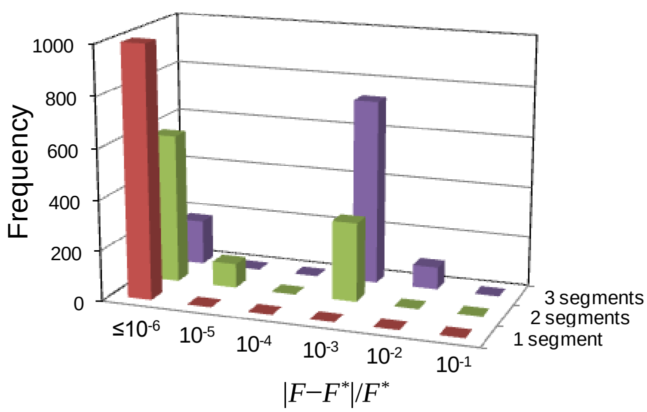

Figure 5. Histogram for the solution errors of 1000 random multi-starts with local NLP solver

4. CONCLUSIONS

We construct an optimization model to determine optimal vehicle design and allocation of conventional, hybrid, and plug-in hybrid vehicles to drivers in order to minimize life cycle GHG emissions. We reformulate the model as a twice-differentiable factorable algebraic nonconvex MINLP that can be solved globally using convexification with a branch-and-reduce algorithm implemented in GAMS/BARON. We find that minimum life cycle GHG emissions can be achieved by assigning a medium-range PHEV36 to drivers who have daily travel distance up to 200 miles. Results indicate that moving drivers from conventional vehicles to HEVs or PHEVs implies significant reductions in life cycle GHGs, but optimal allocation of vehicles to drivers is of second order importance. While larger battery packs may be better for reducing petroleum consumption, larger packs do not necessarily result in lower GHGs, and the best solution is a combination of mid-sized packs that reduce unnecessary GHGs associated with battery production and reduced efficiency due to weight. Grid decarbonization makes larger battery packs more competitive for GHG reduction.

We also compare the solution performance of the random multi-start method to the deterministic global optimization approach. The results indicate that the probability of the multi-start method finding global solution decreases as the number of driver segmentation increases.

Adoption of PHEVs will depend critically on cost. We examine cost and petroleum consumption objectives in a companion paper and examine sensitivity of minimum cost solutions to variation in parameters such as battery prices, fuel and electricity prices, and carbon allowance prices [20]. The global MINLP framework presented here provides confidence in comparing solutions across sensitivity scenarios.

ACKNOWLEDGMENTS

The authors would like to thank Prof. Jay Whitacre, Prof. Chris Hendrickson, Scott B. Peterson, and the members of the Design Decisions Laboratory, the Carnegie Mellon Green Design Institute and Electrified Transportation Group for their feedback and help with model formulation. This research was supported in part by the National Science Foundation's CAREER Award #0747911, a grant from the National Science Foundation program for Material Use, Science, Engineering and Society (MUSES): Award #0628084, and grants from Ford Motor Company and Toyota Motor Corporation. C.-S.S. acknowledges support from the Liang Ji-Dian Fellowship.

REFERENCES

[1] Shiau, C.-S.N., Peterson, S.B., and Michalek, J.J., 2010, "Optimal Plug-in Hybrid Electric Vehicle Design and Allocation for Minimum Life Cycle Cost, Petroleum Consumption and Greenhouse Gas Emissions," *ASME 2010 International Design Engineering Technical Conferences*, DETC2010-28198.

[2] Bandivadekar, A., Bodek, K., Cheah, L., Evans, C., Groode, T., Heywood, J., Kasseris, E., Kromer, M., and Weiss, M., 2008, "On the Road in 2035: Reducing Transportation's Petroleum Consumption and Ghg Emissions," LFEE 2008-05 RP, Massachusetts Institute of Technology, Cambridge, MA.

[3] Frank, A.A., 2007, "Plug-in Hybrid Vehicles for a Sustainable Future," American Scientist, **95**(2), pp. 158-165.

[4] Samaras, C., and Meisterling, K., 2008, "Life Cycle Assessment of Greenhouse Gas Emissions from Plug-in Hybrid Vehicles: Implications for Policy," Environmental Science & Technology, **42**(9), pp. 3170-3176.

[5] Bureau of Transportation Statistics, 2003, "National Household Travel Survey 2001", U.S. Department of Transportation.

[6] Markel, T., Brooker, A., Gonder, J., M. O'Keefe, Simpson, A., and Thornton, M., 2006, "Plug-in Hybrid Vehicle Analysis," NREL/MP-540-40609, National Renewable Energy Laboratory, Golden, CO.
[7] Papalambros, P.Y., and Wilde, D.J., 2000, *Principles of Optimal Design: Modeling and Computation*, Cambridge University Press, New York.
[8] Arora, J.S., Elwakeil, O.A., Chahande, A.I., and Hsieh, C.C., 1995, "Global Optimization Methods for Engineering Applications - a Review," Structural Optimization, **9**(3-4), pp. 137-159.
[9] Conn, A.R., Scheinberg, K., and Vicente, L.N., 2009, *Introduction to Derivative-Free Optimization*, Society for Industrial and Applied Mathematics, Philadelphia, PA.
[10] Tawarmalani, M., and Sahinidis, N., 2002, *Convexification and Global Optimization in Continuous and Mixed-Integer Nonlinear Programming*, Kluwer Academic Publishers
[11] Argonne National Laboratory, 2008, "Powertrain Systems Analysis Toolkit (Psat)."
[12] Shiau, C.S.N., Samaras, C., Hauffe, R., and Michalek, J.J., 2009, "Impact of Battery Weight and Charging Patterns on the Economic and Environmental Benefits of Plug-in Hybrid Vehicles," Energy Policy, **37**(7), pp. 2653-2663.
[13] Environmental Protection Agency, "Dynamometer Drive Schedules", http://www.epa.gov/nvfel/testing/dynamometer.htm.
[14] Peterson, S.B., Whitacre, J.F., and Apt, J., 2010, "Lithium-Ion Battery Cell Degradation Resulting from Realistic Vehicle and Vehicle-to-Grid Utilization," Journal of Power Sources, **195**(8), pp. 2385–2392.
[15] EPRI, 2007, "Environmental Assessment of Plug-in Hybrid Electric Vehicles. Volume 1: Nationwide Greenhouse Gas Emissions," Electric Power Research Institute.
[16] Weber, C.L., Jaramillo, P., Marriott, J., and Samaras, C., 2010, "Life Cycle Assessment and Grid Electricity: What Do We Know and What Can We Know?," Environmental Science and Technology, **44**(6), pp. 1895–1901.
[17] Energy Information Administration, 2008, "Annual Energy Review 2007", U.S. Department of Energy, http://www.eia.doe.gov/emeu/aer/elect.html.
[18] Environmental Protection Agency, 2006, "Emission Durability Procedures and Component Durability Procedures for New Light-Duty Vehicles, Light-Duty Trucks and Heavy-Duty Vehicles; Final Rule and Proposed Rule", http://www.epa.gov/EPA-AIR/2006/January/Day-17/a074.pdf.
[19] Tawarmalani, M., and Sahinidis, N.V., 2004, "Global Optimization of Mixed-Integer Nonlinear Programs: A Theoretical and Computational Study," Mathematical Programming, **99**(3), pp. 563-591.
[20] National Research Council, 2009, *Hidden Costs of Energy: Unpriced Consequences of Energy Production and Use*, The National Academies Press, Washington, DC.

APPENDIX

Table A1. Polynomial coefficients of the PHEV performance meta-model

f_{m3}	η_E	η_G	t_{CD}	t_{CS}	μ_{CD}^*	μ_{CS}^*	u_{CS}^*
m	1	2	3	4	5	6	7
a_{m1}	0.008	2.214	1.457	3.334			
a_{m2}	0.154	1.087	-5.496	-2.266			
a_{m3}	0.353	5.578	-28.46	-20.26			
a_{m4}	-0.005	-0.815	0.913	0.414			
a_{m5}	-0.005	0.510	-0.881	-3.524			
a_{m6}	-0.025	1.562	-1.050	-0.286			
a_{m7}	0.000	2.212	-0.308	-10.11			
a_{m8}	-0.057	-0.613	2.044	1.951			
a_{m9}	-0.043	0.254	15.61	10.31			
a_{m10}	-0.016	-0.159	0.336	5.808			
a_{m11}	-0.001	-8.906	-4.634	-6.932	0.010	0.466	-0.194
a_{m12}	-0.805	-6.095	31.48	15.80	0.011	-0.008	-0.005
a_{m13}	-0.656	-15.21	34.02	39.20	0.053	-0.018	0.047
a_{m14}	0.057	0.089	1.153	7.901	0.000	-0.014	0.000
a_{m15}	0.080	-3.274	1.169	6.582	0.008	-0.038	0.011
a_{m16}	0.342	2.498	-32.06	-30.12	-0.003	0.010	-0.001
a_{m17}	-0.191	2.622	3.405	-6.734	0.097	-0.890	0.382
a_{m18}	1.189	9.285	-54.47	-26.39	0.038	0.077	0.019
a_{m19}	-0.347	5.837	9.570	-4.098	0.370	0.400	-0.077
a_{m20}	4.960	57.68	44.23	32.10	2.196	1.441	0.140

* The terms are fit with quadratic form.